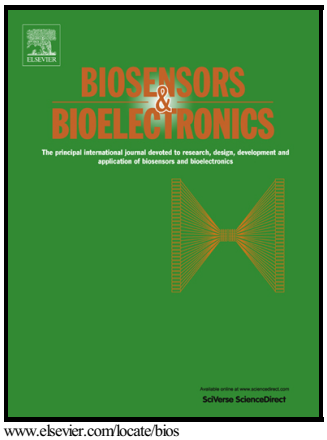

www.elsevier.com/locate/bios

Development of A genosensor for peanut allergen ARA h 2 detection and its optimization by surface response methodology

Marta Sánchez-Paniagua López, Gloria Frutos Cabanillas, M. Jesús Lobo Castañón, Beatriz López-Ruiz

PII: S0956-5663(14)00488-6
DOI: http://dx.doi.org/10.1016/j.bios.2014.06.065
Reference: BIOS6899

To appear in: *Biosensors and Bioelectronic*

Received date: 4 July 2014
Revised date: 4 July 2014
Accepted date: 4 July 2014

Cite this article as: Marta Sánchez-Paniagua López, Gloria Frutos Cabanillas, M. Jesús Lobo Castañón and Beatriz López-Ruiz, Development of A genosensor for peanut allergen ARA h 2 detection and its optimization by surface response methodology, *Biosensors and Bioelectronic,* http://dx.doi.org/10.1016/j.bios.2014.06.065

DEVELOPMENT OF A GENOSENSOR FOR PEANUT ALLERGEN ARA H 2 DETECTION AND ITS OPTIMIZATION BY SURFACE RESPONSE METHODOLOGY

Marta Sánchez-Paniagua López[1], Gloria Frutos Cabanillas[2], M. Jesús Lobo Castañón[3], Beatriz López-Ruiz[1*]

[1]Departamento de Química Analítica, Facultad de Farmacia, Universidad Complutense, Pz. Ramón y Cajal s/n, 28040 Madrid, Spain.

[2]Departamento de Estadística e Investigación Operativa, Facultad de Farmacia, Universidad Complutense, Pz. Ramón y Cajal s/n, 28040 Madrid, Spain.

[3]Departamento de Química Física y Analítica, Universidad de Oviedo, c/ Julián Clavería 8, 33006 Oviedo, Spain

*To whom correspondence should be addressed.

bealopru@ucm.es

Abstract

A new selective electrochemical genosensor has been developed for the detection of an 86-mer DNA peanut sequence encoding part of the allergen Ara h 2 (conglutin-homologue protein). The method is based on a sandwich format, which presents two advantages: it permits shortening the capture probe and avoids labeling of the target. Screen-printed gold electrodes have been used as platform for the immobilization of oligonucleotides by the well-known S-Au bond. Mixed self-assembled monolayers (SAM), including thiol-modified capture probe and mercaptohexanol, were prepared to achieve an organized, homogeneous and not too compact SAM in which unspecific adsorption of the capture probe would be prevented. The optimization of the sensing phase was carried out using the Design of Experiments (DoE) approach. Traditionally, response optimization is achieved by changing the value of one factor at a time until there is no further improvement. However, DoE involves regulating the important factors so that the result becomes optimal. Optimized conditions were found to be 1.34 μM for capture probe concentration and 3.15 mM for

mercaptohexanol (spacer) concentration. When the optimal conditions were employed the analytical performance of the proposed genosensor improved significantly, showing a sensitivity as high as 3 μA/nM, with a linear range from $5 \cdot 10^{-11}$ to $5 \cdot 10^{-8}$ M and a detection limit of 10 pM.

Keywords: Electrochemical genosensor, self-assembled monolayers, Ara h 2 peanut allergen, Design of Experiments.

1. INTRODUCTION

Peanut is a widespread ingredient in food industry, causing severe allergic reactions to a growing sector of the population. These allergic sufferers must follow a lifelong peanut-free diet. Although the threshold level required to cause the allergic reaction is not known with certainty, there are studies showing that micrograms of protein are enough to produce allergic reactions in hypersensitive subjects (Morisset et al., 2003). According with the study reported by Bock et al. (Bock et al., 2001) most of the fatal anaphylactic reactions to foods seem to be caused by peanuts. Therefore, to protect all the peanut allergic consumers and to ensure compliance with the European legislation on food labeling, which includes peanuts among the 14 food allergens to be labeled on pre-packed foods regardless of its content, there is a clear need for sensitive, efficient and reliable methods for the detection of peanut allergens in food.

Two different approaches have been used for the determination of the allergen content in foods: protein-based and DNA-based methods (Hefle et al., 2006). The first group detects some of the allergenic peanut protein while the latter is based on the detection of oligonucleotide sequences that encode any of these allergenic proteins. (Pomés et al., 2003; Stephan et al., 2004; Zeleny et al., 2010). Unfortunately, commercial production processes involve a heat treatment that can denatures proteins. Therefore, DNA-detection technology has been developed as an alternative for these purposes. Different methods based on real-time Polymerase Chain Reaction have been described for peanut DNA detection (Hird et al., 2003, Watanabe et al., 2006; Lopez-Calleja et al., 2012). However, most of them are time-

consuming and require expensive equipment. Genosensors have irrupted as a new DNA-detection technology due to their simplicity, automatization, low cost, and selectivity. Despite the positive attributes of these devices, its application to the detection of DNA sequences encoding peanut allergens is very limited, with a recent work describing an impedimetric genosensor for detecting a DNA sequence specific of Ara h.1 (Sun et al., 2012)

Peanut contains two allergens that are recognized by over 90 % of peanut-allergic adults, the Ara h 1 (vicilin family) and the Ara h 2 (conglutin family) (Hefle, 2006). Although the protein Ara h 1 (vicilin family) accounts for about 20% of the total peanut proteins, Ara h 2 (conglutin family) constitutes the most frequently recognized allergen in children (Nicolaou et al., 2005; Flinterman et al., 2007). In the present work, an electrochemical genosensor for detection of an 86-mer DNA sequence encoding part of the allergenic protein Ara h 2 from peanut, was developed. This sensor is based on a sandwich format, which allows shorten the capture probe and improve selectivity while avoiding the labeling of the target. Screen-printed gold electrodes have been used as platform for the immobilization of the capture probe, complementary to the 3'-end of the target, by the well-known S-Au bond, followed by the chemisorption of mercaptohexanol as a blocker resulting in a mixed self-assembled monolayer (SAM) (Carpini 2004). The optimization of the composition of the sensing phase is critical to get the best analytical performance. Despite the Design of Experiments (DoE) approach has proved to be a powerful tool in Analytical Chemistry (Montgomery, 2009), and especially in optimizing analytical devices, their use has not become widespread in the field of biosensors (Rubio Retama et al., 2005; Alonso-Lomillo et al., 2010; Venturin et al., 2011). This study has been focused on the optimization of the sensing phase using DoE approach to achieve an organized, homogeneous and not too compact SAM in which unspecific adsorption of the capture probe could be prevented.

2. EXPERIMENTAL

2.1. Reagents

Dithiothreitol (DTT), 6-Mercapto-1-hexanol (MCH), streptavidin-alkaline phosphatase ($Strp_2$-ALP), 1-naphthyl phosphate, bovine serum albumin (BSA), Tween 20, salts for buffer solutions (Tris, $MgCl_2$) and the saline sodium phosphate solution, 20×SSPE (200 mM sodium phosphate, 3 M NaCl, 20 mM EDTA), pH 7.4 were obtained from Sigma-Aldrich (Spain). Ethanol and sulfuric acid were purchase from Panreac (Spain). Three buffer solutions were used: i) immobilization and hybridization buffers (2×SSPE, pH 7.4), ii) blocking buffer (5×SSPE, pH 7.4 containing 5% w/v BSA and 0.1% Tween 20), and iii) measurement buffer (0.5M Tris-HCl, pH 9.8, 1mM $MgCl_2$, 0.1 M KCl).

Oligonucleotide sequences used were purchased from Sigma-Life Science as lyophilized desalted salts, (Table S1). In order to immobilize the capture probe on the gold screen printed electrode, the 5' end of the sequence was functionalized with a thiol group. The stock solutions were prepared in Milli-Q water and stored at -20ºC. The thiol-modified capture probe was commercially supplied as the respective disulfide. To reduce the S-S bonds and obtain the SH terminal groups, prior to use, a treatment with 0.1 M DTT for 16 h at room temperature was required. The resulting thiol-sequence was purified by elution through a Sephadex G25 column (NAP-10, Pharmacia Biotech) with Milli-Q water. The concentration of the stock solutions were checked spectrophotometrically at 260 nm before stored at -20 °C.

2.2. Instrumentation

Electrochemical measurements were carried out with screen-printed gold electrodes (SPEAu, DropSens-220BT, Spain), connected to a μ-AutoLab PGSTAT12 potentiostat with GPES 4.9 software (EcoChemie, The Netherlands). The layout of the disposable planar screen-printed gold electrodes includes three electrodes in the same alumina sheet: a working gold electrode (Ø ~ 4 mm), an Ag pseudo-reference electrode and a gold counter electrode. A specific connector supplied by DropSens acts as interface between the screen-printed cell and the potentiostat. The experiments were carried out at room temperature (20ºC) and a new screen-printed electrode was used for each assay. The pH measurements were performed on a

Crison micropH 2001 pHmeter (Spain). Spectrophotometric measurements were carried out with a UV-visible Cary 300 Bio spectrophotometer (Tehcnologies Agilent, USA).

2.3. Analytical Procedures

Electrode pretreatment

First, screen-printed electrodes were washed with water and ethanol and dried with nitrogen. After that electrodes were conditioned to improve the sensitivity and reproducibility by an electrochemical pretreatment of 25 cyclic voltammetric scans between 0 and 1.6 V at 100 mV s^{-1}, in a 0.5 M H_2SO_4 solution, until a stable cyclic voltammogram was obtained. Before being modified, electrodes were washed again with water and dried with nitrogen.

Sensing phase

The sensing interface consists of a SAM onto gold screen-printed electrodes containing a linear capture probe and MCH as diluent. Firstly, 15 µL of the thiolated capture probe solution was placed onto the clean gold working electrode surface and kept at 4 ºC for a fixed time, as a result of this step the capture probe is attached to the electrode surface by the SH-end, afterwards the electrode was rinsed with the immobilization buffer to remove the weakly adsorbed DNA, (Figure 1, Step 1). Unfortunately, after this stage a disordered monolayer results due to the non-specific adsorption of nucleotidic bases to the surface electrode.

More precise control over the coverage of the gold surface was achieved by creating a mixed monolayer of the thiol-capture probe and a short alkanethiol as spacer, MCH, using a two-step method. In a second step 10 µL of MCH solution was added on the surface electrode for a time, followed by further rinsing with 2×SSPE buffer.

Sandwich assay

Hybridization assay was performed in a sandwich format that requires two steps, a homogeneous followed by a heterogeneous hybridization. In the first step, the homogeneous hybridization reaction between a biotinylated-signaling probe and the

target takes place in the hybridization buffer solution, (Figure 1, Step 2). In this process, the solution was heated at 95ºC for 5 min and cooled in an ice-water bath for 5 min, and afterwards it was left at 25ºC for a period of time. Immediately, 15 µL of the resulting solution was placed on the modified electrode at room temperature, so that the heterogeneous hybridization reaction takes place (Figure 1, Step 3). Finally, the working electrode was rinsed with the hybridization buffer to remove nonspecifically adsorbed sequences.

Electrochemical detection

To achieve the electrochemical detection an enzyme labeling was chosen; the conjugate streptavidin-alkaline phosphatase was used for this purpose (Figure 1, Step 4). Before the addition of the enzyme label, in order to minimize the non-specific adsorption of the complex streptavidin-alkaline phosphatase onto the electrode, the electrode was covered with the blocking buffer for 10 min and afterwards 15 µL of a solution of $Strp_2$-ALP in blocking buffer was added to the sensor. Later the sensor was washed with the blocking buffer. The amount of enzyme bound to the electrode was monitored by differential pulse voltammetry. After 10 min of incubation in a 1-naphthyl phosphate solution prepared in 0.5 M Tris-HCl pH 9.8 containing 1 mM $MgCl_2$, DPV voltammograms were registered from 0 to 0.6 V, modulation amplitude 50 mV and scan rate 10 mV s^{-1}, for measuring the 1-naphthol generated after enzymatic dephosphorylation, (Figure 1, Step 5). The experiments were carried out at room temperature and a new screen-printed electrode was used for each assay.

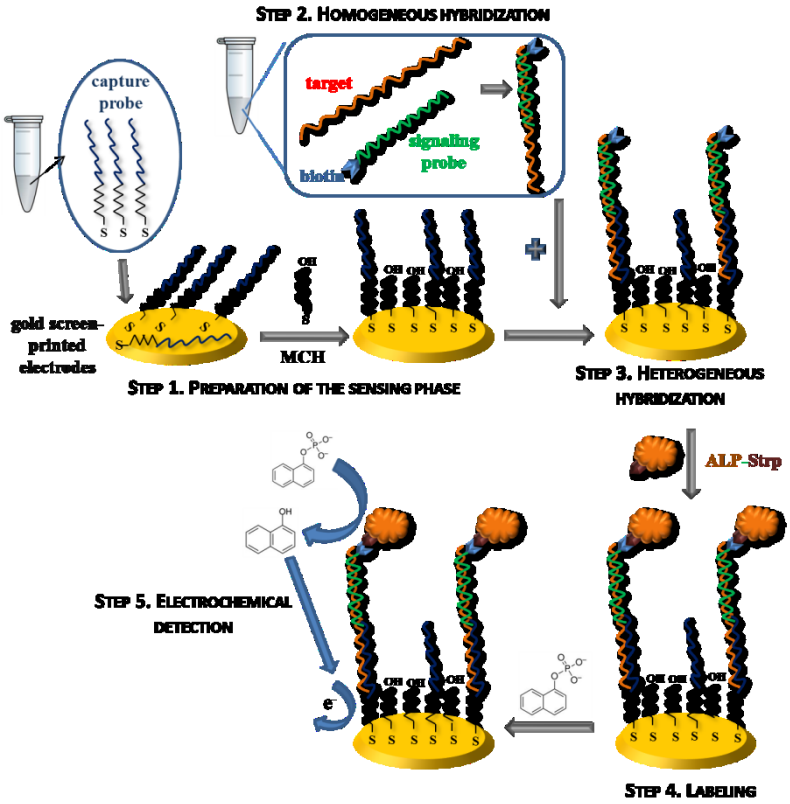

Figure 1. Genosensor scheme.

2.4. Statistical procedures

Statistically, DoEs has been used to improve and optimize the performance of the new genosensor (Box et al., 2005). A sequential Response Surface Methodology (RSM), consisting of the following general phases, *i*) *screening*, *ii*) *modeling* and *iii*) *optimization*, has been applied (Box et al., 1957; Myers et al., 2008). *i*) First, a Plackett-Burman (Plackett et al., 1946) design of thirteen factors, each at two levels, has been carried out with n experiments ($n = 2^{13} \cdot 5/2048=20$). The factor and their levels are shown in Table 1. The screening experiments are designed to achieve early detection of the control factors that produce the biggest impact on the response (current intensity) and their optimal range. In order to obtain a deeper knowledge about the sensing phase, a second screening design, 2^5 factorial, has been performed. *ii*) With the purpose of modeling the response as a function of the two factors selected from the previous 2^5 design, experiments have been carried out according to factorial design 3^2. *iii*) Finally, a Multiple Response Optimization has

been applied in order to combine the two responses into a single function that can be maximized, using graphical and numerical optimization. The Overlaid Contour Plots is a graphical optimization method that simply consists of overlaying contour plot for each of the responses one over the other in the controllable factors space and to find the area with the best possible values for each of the responses. The Desirability Function approach has been used, this is a numerical optimization based on a transformation of the response into a range of values between 0 and 1 (Derringer, G. et al., 1980). This transformed response, called d_i, can have many different shapes. Regardless of the shape, a response of 0 represents a completely undesirable response and 1 represents the most desirable response. In order to simultaneously optimize several responses, each of these d_i are combined using a weighted geometric mean defined as overall desirability

$$D = \quad d_1^{\,w_1}\, d_2^{\,w_2} \ldots\ldots\ldots\ d_p^{\,w_p}{}^{\,1}{}_{\,i} w_i$$

where d_i is the individual desirability function of the *i*-th response (*i* = 1, 2, …, *p*) and w_i are user-specified weights to assign priorities to d_i.

The analytical responses have been processed using the Statgraphics Data Analysis Package Centurion Version XVI (STATGRAPHICS® 2010).

Table 1.- Screening design including the selected thirteen factors with their levels and physical units.

GENOSENSOR STEPS	FACTORS	LEVELS		UNITS
		LOW	HIGH	
Step 1: Sensing phase	A: cCP	0.2	4.0	μM
	B: tCP	1.0	19	h
	C: ISI	0.36	0.9	M
	D: cMCH	0.5	4.5	mM
	E: tMCH	10.0	60.0	min
Step 2: Labeling	F: cSP	0.2	4.0	μM
	G: cT	1.0	100.0	nM
	H: tHHo	1.0	30.0	min
	I: ISH	0.36	0.90	M
Step 3: Measurement	J: tHHe	0.25	4.0	h
	K: cE	0.5	4.3	mg/L
	L: tE	15.0	45.0	min
	M: cNP	0.4	4.0	mM

3. Results and discussion

3.1. Genosensor design

The scheme of the genosensor is depicted in Figure 1. A disposable screen printed gold electrode was selected. Regarding the choice of target and probes different aspects must be taken into account. Firstly, the base sequence chosen as target must be specific of peanut and as short as possible to minimize the risk of strong secondary structures that would hinder the hybridization process (Del Giallo et al. 2005). Since the same base sequence can be present in different genes, a detailed

study on the specificity of the target sequence was done. An 86 base sequence from the gene encodingthe allergen Ara h 2 (GenBank accession number L77197) was chosen as target (Fig.2.a). The specificity of this sequence was controlled withBLAST software (Basic Local Alignment Search Tool) [http://www.ncbi.nlm.nih.gov/blast].

A sandwich assay format was performed, using two single-stranded fragments contiguous and complementary to the target, the capture and the signaling probes. This type of assay has two important advantages, it allows the denaturation of the target and signaling probe by thermal treatment before homogeneous hybridization takes place and also permits the use of shorter capture probes giving as a result more organized sensing phases. A 5´ thiolated capture probe (32 nucleotides) (Fig.2.b) and a signaling probe functionalized at its 3' end with biotin (54 nucleotides) (Fig. 2.c) were designed; both sequences are entirely complementary to part of the target, forming a perfect and rigid duplex. Mfold Web Server was used to predict the secondary structures of the designed sequences (Figure 2) (Zuker, 2003). The target is predicted to have a very stable secondary structure (ΔG = -16.71 kcal / mol) at 20ºC. The capture probe, signaling probe, target-capture probe hybrid and target-signaling probe hybrid present ΔG values of -2.9 kcal/mol, -4.39 kcal/mol, -49.8 kcal/mol and -85.5 kcal/mol, respectively. These data demonstrate the spontaneous hybridization between the target and both probes.

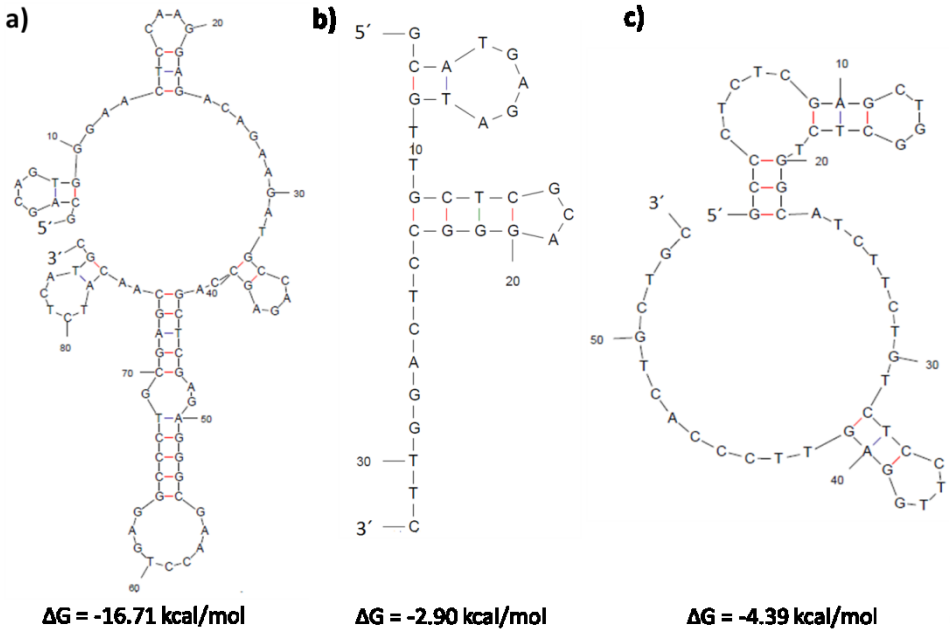

Figure 2. Possible folding of (a) target, (b) capture probe and (c) signaling probe DNA single strands as calculated using Mfold Webserver software.

3.2. Screening experimental design

As it is well known, sensor response could be affected by a large number of variables. Plackett-Burman experimental design is an efficient screening method, which requires few experimental runs and allows identifying the control factors when complete knowledge of the system is unavailable. This design is a fractional design with 2 levels and resolution III, which has complicated confounding relationship between the main effects and the two-factor interactions effects. Nevertheless this screening design provides a general idea about which factors are the dominant ones, and their ranges.

The graphical results obtained by the Plackett-Burman design are presented in Figure S1, in which Pareto plot (Fig. S1.a) shows the main effects, and the Normal probability plot (Fig. S1.b) shows the standardized effects for the factors.

Due to the resolution III of the Plackett-Burman design, no variables could be excluded, but an optimization process with thirteen variables becomes impracticable,

(2^{13} = 8192). Therefore, a deeper study of each step of the sensor is required. Considering that the composition and structure of the sensing phase is of crucial importance in the performance of the genosensor, the study started by the optimization of this step.

3.3. Sensing phase optimization

In order to know the main effects and the two factor interactions, two 2^5 factorial designs (*Signal* and *Blank*) were constructed, including the experimental variables involved in the sensing phase preparation at two levels (Table 1). 64 genosensors were constructed by the same analyst and the same day, using a new electrode in each experience (Table S2); half of them were evaluated in the presence of a concentration of the target 10 nM (*Signal*) and the other half were used for the measurement of the response in the absence of the target (*Blank*). According to additional experiences, the rest of factors were held constant at the following values, 2 μM of cSP in a 0.9 M ISH, as tHHo 30 min at 25ºC after 5 min at 95ºC and 5 min in ice-water, as tHHe 2 h, 1.075 mg/L of cE, 30 min of tE and 4 mM of cNP.

According to the statistics summary obtained, the 32 *Signal* values ranged from 0.65 μA to 8.94 μA, the mean value was 4.42 μA and the coefficient of variation was 47.23% (considerably less than that obtained with the screening design).*Blank* values ranged between 0.077μA and 0.62 μA, the mean value was 0.25 μA with a coefficient of variation of 72.27 %. This excessive dispersion suggests that changes in the mixed monolayer composition induce great relative changes in the *Blank*. Figure S2 shows the standardized Pareto plots for the *Signal* (with target), *Blank* and the new variable generated, S*ignal/Blank*.

The negative effect of ionic strength in the *Blank* (it increases with decreasing ionic strength) could be explained by the effect of the cations from the inert salts on the negatively charged DNA sequences; cations neutralize the charge of the strands, preventing the electrostatic repulsion between them. As a result, at high ionic strength a monolayer much more organized is achieved, minimizing the non-specific adsorption events. The positive effect on the *Signal* could be explained by the fact

that the hybridization reaction improves when the electrostatic repulsion between the complementary strands has been minimized.

According to Pareto plots, although the tCP has a positive effect in the response for both *Signal* and *Blank*, the effect on the *S/B* ratio is practically negligible. About the MCH immobilization time, it showed an insignificant effect on the ratio *S/B* and no significant effect on the *Signal* and *Blank*.

The cCP has a clear negative effect in the *Blank*, while its effect on the *Signal* appears to be positive. Concerning the cMCH, although its main effect on the *Signal* and *Blank* is really small, its interaction effect with the cCP (interaction AD) is significantly higher in both cases.

The optimization of the sensing phase requires a factorial design at three levels or a composite design able to detect curvatures in responses. To perform these designs, it must be consider the minimum number of factors. Hence, some of these factors must be excluded. In order to found the optimal working conditions, i.e., minimal *Blank* and maximum *Signal*, the influence of cCP and cMCH has to be evaluated on a new DoE but the rest of the variables must be eliminated from the design and kept at a fixed value.

The large effect of the ionic strength might hide the effects of the rest of variables. Therefore, this variable has to be removed from the design and kept constant. In order to establish its most appropriate value, we individually studied the influence of the ionic strength of the CP solution during immobilization on the sensor response. The current measured for a target concentration 10 nM increases up to a maximum value corresponding to immobilizations carried out in 0.9 M (Figure S3). In lower ionic strength solutions, less probe immobilization occurs because of the larger electrostatic repulsion between the strands, whereas in high ionic strength solutions the electrostatic repulsions between probes are effectively minimized and higher probe density can be reached. But, when the electrode coverage of capture probe is too high, a decrease in the surface hybridization could be produced. (Peterson et al., 2001). So, to achieve the highest efficiency in immobilization, an ionic strength of 0.9 M was used in the following experiments.

Remarkably, when tCP was increased a significant increase in the reproducibility was found, RSD= 9% for 19 h, RSD= 16% for 10 h and RSD=18% for 1 h for 8 independent measurements. Therefore, in further studies tCP was fixed in 19 h. Finally, the tMCH appears to have a negative effect on the *Signal* and positive on the *Blank,* with an insignificant effect on *S/B* ratio. So, to obtain the highest response in the shortest time this factor was fixed in 15 min. These factors were excluded from the design and kept at the referred.

Once most of the factors were excluded from the design, as explained above, we evaluated the influence of cCP and cMCH using a new DoE. With this aim two 3^2 factorial designs were performed to estimate the responses for *Signal* for 10 nM cT and *Blank* as quadratic functions of cCP and cMCH. Results are shown in Table S3.

Statistics summary informs that the nine *Signal* values ranged between 1.640μA and 17.2μA with a mean value of 10.764μA and coefficient of variation of 47.71%; the nine *Blank* values were ranged between 0.252μA and 0.765μA, the mean value was 0.414μA and coefficient of variation was 35.10%.

The analysis of the results for the *Signal* (Figure S4), shows that the quadratic effects of both factors and their interaction are statistically significant (a), the main effects are quadratic (b), there is a clear interaction between the quadratic effects of cCp and cMCH (c), the most important effects correspond to $cMCH^2$ and cCP×cMCH (d), and the response surface (e) presents a maximum value (f) of 15.82 μA reached at cCP = 1.02 μM and cMCH = 2.70 mM. ANOVA for *signal* probes that the quadratic effect of the factors (A^2 and B^2) and the interaction between the factors (AB) are significantly different from zero at the 95.0% confidence level (*p*-values equal to 0.0014, 0.0063 and 0.0045, respectively). The fitted model is given by the equation,

$$Signal = 5.23 + 4.98 \times cCP + 5.98 \times cMCH - 4.50 \times cCP^2 + 1.55 \times cCP \times cMCH - 1.40 \times cMCH^2$$

where the values of the variables are specified in their original units. The goodness of the fit measures indicates that the fitted model is suitable: coefficient of determination (R^2 =0.9789), the standard error of the estimate (SE = 11.1876), the average value of the residuals (5.5867) and finally the Durbin-Watson statistic residual test (*p*-value = 0.4987).

When the same analysis is performed for *Blank* (Figure S5), we observed that the linear effect for cMCH is statistically significant (a), main effects are nonlinear (b), there is no interaction between the quadratic effects of cCp and cMCH (c), the most important effects correspond to cMCH and cCP (d), and the response surface (e) presents a minimum value (f) of 0.25 µA reached at cCP = 2.00 µM and cMCH = 3.23 mM. The ANOVA for *blank* probes that only the cMCH (B) is significantly different from zero at the 95.0% confidence level (*p*-value = 0.0114). The equation of the fitted model is given by the equation,

$$Blank = 0.84 - 0.15 \times cCP - 0.22 \times cMCH - 0.\ 012 \times cCP^2 + 0.03 \times cCP \times cMCH + 0.02 \times cMCH^2$$

where the values of the variables are specified in their original units. The goodness of the fit measures indicates that the fitted model is suitable: coefficient of determination (R^2 =0.8878), the standard error of the estimate (SE = 0.0729), the average value of the residuals (0.4056) and finally the Durbin-Watson statistic residual test (*p*-value = 0.8554).

Multiple Response Optimization

This procedure determines the combination of experimental factors which simultaneously optimize several responses. In that study *Signal* and *Blank*. Figure 3 shows the following results: (a) response surface for desirability function; (b) overlay contour plots for each response, the striped area shows the range for cCP and cMCH where the criteria for both response variables are satisfied; (c) the upper table shows the combination of factor levels which maximize the desirability function over the indicated region, and the bottom table shows, the combination of the factors at which that optimum is achieved. Optimize conditions were found when the sensor was prepared from 1.34 µM cCP and 3.15 mM cMCH, quite far from the conditions commonly used in similar devices, which are around 0.5 µM cCP and 2 mM cMCH.

a)

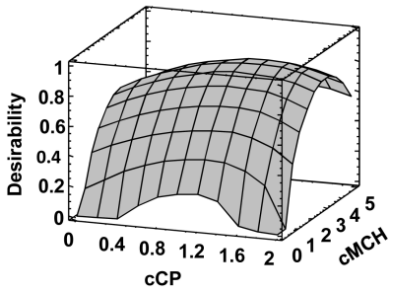

b)

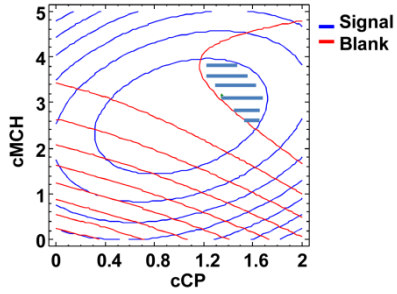

c) Optimized Conditions

Factor	*Low*	*High*	*Optimum*
cCP	0.1	2.0	1.34
cMCH	0.5	4.5	3.15

Response	*Optimum*
Signal	15.28
Blank	0.31

Figure 3. a) Response surface for desirability function b) overlay contour plots for each response, *Signal* and *Blank*, and c) optimal conditions for cCP and cMCH (upper table) and optimal values for the responses (bottom table).

3.4. Calibration curve, selectivity and reproducibility

A calibration curve was performed under the established optimal conditions: cCP 1.35 µM and cMCH 3.15 mM, 0.9 M of ISH, 15 min of tMCH, 19 h of tCP, 2 µM of cSP, tHHo 30 min at 25ºC (this step is preceded by a denaturation at 95ºC for 5 min followed by 5 min in ice-water), tHHe 2 h, 1,075 mg/L of cE, 30 min of tE and 4 mM of cNP. Figure 4.a shows DPV signals for different concentrations of target and the blank. Figure 4.b. shows the calibration curve, a linear response in the range of $5{\cdot}10^{-11}$ to $5{\cdot}10^{-8}$ M was obtained (inlet) and the regression equation was $I(A) = (1{\cdot}10^{-7} \pm$

$8 \cdot 10^{-9}$) + ($3 \cdot 10^{-6} \pm 2 \cdot 10^{-7}$) × C(nM) ($r$ = 0.998, n=3). A detection limit, estimated as the concentration that gives a signal equal to the blank media plus three times the standard deviation of the blank $x_B + 3\sigma_B, N = 10$ was found to be 10 pM. Selectivity was evaluated by comparatively testing the response towards 1 nM of target, 1 nM of a non complementary sequence (nC) and 1 nM of a three-base mismatched DNA sequence (Table S1). A negligible signal was observed with the nC sequence and the mismatched sequence gave a 24 % of the signal registered with the target (Figure 4.a, inlet). Eight parallel-made DNA sensors were used to detect 10 nM of target DNA obtaining a RSD of 7.22 %. These results probe the suitable genosensor reproducibility.

Under these conditions the genosensor showed a much higher sensitivity and lower detection limit than the achieved by classical one-to-one approach which are around 1 μA/nM and 0.1 nM respectively (Martín-Fernández et al. 2014).

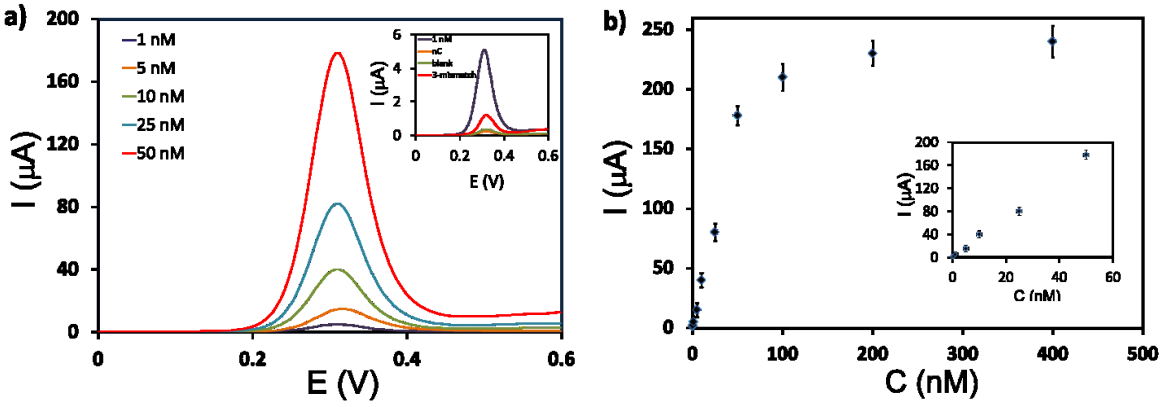

Figure 4. a) DPV voltamperograms from different cT (1, 5, 10, 25 and 50 nM). Inlet: DPV voltamperograms from blank, a non-complementary sequence (nC), 1nM, a three mismatched DNA sequence, 1nM and target, 1 nM. Scan rate 10 mV s^{-1}, pulse amplitude 20 mV. b) Calibration curve under the optimum conditions. The linearity range is plotted in the inlet.

4. Conclusions

The analytical performance of the sensor was significantly improved by means of the RSM methodology. The optimized conditions were found using the desirability function approach.

A selective electrochemical genosensor for detecting allergen Ara h2 was developed, with higher sensitivity and lower detection limit than the achieved by classical one-to-one approach.

The DoEs provides a satisfactory tool for this kind of devices.

5. Acknowledgements

This work has been cofinancied by Project CTQ2008-02429/BQU granted to “Grupos Consolidados”, CTQ2012-31157 and the European Regional Development Fund.

Abbreviations

BSA Bovine serum albumin

cCP Capture probe concentration

cE Strp-ALP concentration

cMCH: MCH concentration

cNP Naphtylphosfate concentration

cSP Signaling probe concentration

cT Target concentration

DoE Design of Experiments

ISH Ionic strength of hybridization

ISI Ionic strength of immobilization

RSM Response Surface Methodology

SAM Self-assembled monolayers

Strp2-ALP Streptavidin-alkaline phosphatase

tCP Capture probe immobilization time

tE Enzymatic labeling time

tHHe Hybridization time (tHHe)

tHHo Hybridization time

tMCH MCH immobilization time

References

Alonso-Lomillo, M.A., Dominguez-Renedo, O., Ferreira-Goncalves, L., Arcos-Martinez, M.J., 2010. Biosens. Bioelectron. 25, 1333-1337.

Bock, S.A., Muñoz-Furlong, A., Sampson, H.A., 2001. J. Allergy Clin. Immun. 107, 191-193.

Box, G.E., Hunter, W.G., Hunter, J.S., Hunter, W.G., 2005. Statistics for Experimenters: Design, Innovation, and Discovery, 2nd Edition, John Wiley & Sons, Inc. Publication. Hoboken. New Jersey.

Box, G.E., Hunter, J.S., 1957. Ann. Math. Stat. 28, 195-241.

Burks, A.W., Cockrell, G., Stanley, J.S., Helm, R.M., Bannon, G.A., 1995. J. Clin. Invest. 96, 1715-1721.

Carpini, G., Lucarelli, F., Marazza, G., Mascini, M., 2004. Biosens. Bioelectron. 20, 167-175.

Del Giallo, M.L., Lucarelli, F., Cosulich, E., Pistarino, E., Santamaria, B., Marrazza, G., Mascini, M., 2005. Anal. Chem. 77, 6324-6330.

Derringer, G., Suich, R., 1980. J. Qual. Technol. 12, 214-219.

Flinterman, A.E., van Hoffen, E., den Hartog Jager, C.F., Koppelman, S., Pasmans, S.G., Hoekstra, M.O., Bruijnzeel-Koomen, C.A., Knulst, A.C., Knol, E.F., 2007. Clin. Exp. Allergy. 37, 1221-1228.

Hefle, S., 2006. Methods for detecting peanuts in food, in: Koppelman, S.J., Hefle, S.L. (Eds.), Detecting allergens in food. Woodhead Publishing Limited, Cambrige, pp. 185-186.

Hird, H., Lloyd, J., Goodier, R., Brown, J., Reece, P., 2003. Eur. Food Res. Technol. 217, 265-268.

Lopez-Calleja, I.M., de la Cruz, S., Pegels, N., Gonzalez, I., Garcia, T., Martin, R., 2012. Food Control 30, 480-490.

Martín-Fernández, B., Miranda-Ordieres, A.J., Lobo-Castañón, M.J., Frutos-Cabanillas, G., Santos-Alvarez, N., López-Ruiz, B., 2014. Biosens. Bioelectron. 60, 244-251.

Montgomery, D.C., 2009. Design and Analysis of Experiments; John Wiley & Sons, Inc. Publication. Hoboken. New Jersey.

Morisset, M., Moneret-Vautrin, D.A., Kanny, G., Guenard, L., Beaudouin, E., Flabbee, J., Hatahet, R., 2003. Clin. Exp. Allergy. 33, 1046-1051.

Myers, R., Montgomery, D., Anderson-Cook, C., 2008. Response Surface Methodology: Process and Product Optimization Using Designed Experiments, 3th Ed. John Wiley & Sons, Inc. Publication. Hoboken. New Jersey.

Nicolaou, N., Poorafshar, M., Murray, C., Simpson, A., Winell, H., Kerry, G., Härlin, A., Woodcock, A., Ahlstedt, S., Custovic. A., 2010. J. Allergy Clin. Immunol. 125, 191-197.

Peterson, A.W., Heaton, R.J., Georgiadis, R.M., 2001. Nucleic Acids Res. 29, 5163-5168.

Plackett, R.L., Burman, J.P., 1946. Biometrika 33, 305-325.

Pomés, A., Helm, RM., Bannon, GA., Burks, AW., Tsay, A., Chapman, MD., 2003. J. Allergy Clin. Immun. 111, 640-645.

Rubio Retama, J., Sanchez-Paniagua, M., Hervas Perez, JP., Frutos Cabanillas, G., Lopez-Cabarcos, E., Lopez-Ruiz, B., 2005. Biosens. Bioelectron. 20, 2268-2275.

STATGRAPHICS® *Centurion* XVI 2010 by StatPoint Technologies, Inc. www.STATGRAPHICS.com. Printed in the United States of America.

Stephan, O., Vieths, S., 2004. J. Agr. Food Chem. 52, 3754-3760.

Sun, X., Guan, L., Shan, X., Zhang, Y., Li, Z., 2012. J. Agric. Food. Chem. 60, 10979-10984.

Watanabe, T., Akiyama, H., Maleki, S., Yamakawa, H., Iijima, K., Yamazaki, F., 2006. J. Food Biochem. 30, 215-233.

Zeleny, R., Schimmel, H., 2010. Food Chem. 123, 1343-1351.

Zuker, M., 2003. Nucleic Acids Res. 31, 3406-3415.

Highlights

- A selective genosensor for peanut allergen, Ara h 2 detection is developed.
- DoEs has proved to be a powerful tool in genosensor performance optimization.
- Multiple Response Optimization is applied in order to combine signal and blank into a single function, desirability function that has been maximized.

FIGURES

Graphical abstract